Midinfrared quantum cascade detector with a spectrally broad response

Daniel Hofstetter,[1,a)] Fabrizio R. Giorgetta,[1,b)] Esther Baumann,[1,b)] Quankui Yang,[2] Christian Manz,[2] and Klaus Köhler[2]

[1] *Institute of Physics, University of Neuchâtel, 1 A.-L. Breguet, CH-2000 Neuchâtel, Switzerland*
[2] *Fraunhofer Institute of Applied Solid State Physics, Tullastrasse 72, Freiburg D-79108, Germany*

A midinfrared quantum cascade detector with a spectrally broad ($\Delta E/E = 27.3\%$) response is designed, fabricated, and tested. This detector consists of 26 differently designed active region stages in order to cover a wavelength region from 4.7 to 7.4 μm. The device could be operated above room temperature and showed peak responsivities of 13 mA/W at 10 K and 1.25 mA/W at room temperature. A background limited detectivity of 1.55×10^{10} Jones was seen up to a temperature T_{BLIP} of 110 K.

During the past couple of years, quantum cascade detectors (QCDs) have experienced a rapid development. Prototype QCDs have been demonstrated in several material systems such as GaAs/AlGaAs,[1,2] InGaAs/InAlAs,[3,4] and InGaAs/AlAsSb,[5] and they cover nowadays a large range of wavelengths spanning from the far infrared (84 μm) (Ref. [6]) down to the near infrared at 2.1 μm.[5] High frequency operation of QCDs up to 23 GHz has been demonstrated in an optical heterodyne experiment using quantum cascade laser sources.[3] Most recent QCDs reached also very decent performance levels, especially in terms of detectivity.[7,8] Most of this promising progress in performance seems to be the result of the optical bound-to-bound transition, which is at the origin of the detection mechanism: it leads to a very narrow spectral linewidth and thus to a substantial reduction of the blackbody background noise seen by the device. In addition, the absence of dark current and thus dark current noise has a positive effect on the noise behavior of these devices. Unfortunately, it was up to now not clear whether a device with a spectrally broad response would—at least partially— preserve the good noise properties of the standard narrow linewidth QCD. Furthermore, it was speculated that monochromatic illumination of a spectrally broad QCD could lead to poor performance, especially at low operating temperatures. In this article, we therefore present a midinfrared QCD with a relative linewidth of 27.3%, which makes use of 26 carefully designed active region stages spanning a wavelength range between 4.7 and 7.4 μm. Despite the large detection spectrum, the noise properties of this device were not too adversely affected: we achieved a background limited detectivity of 1.55×10^{10} Jones up to a temperature T_{BLIP} of 110 K.

Fabrication of this device relied on molecular beam epitaxy on an Fe-doped InP substrate. The layer structure is based on 26 stages all having a similar architecture. The main well of each stage is n-doped and contains a ground state plus an excited state. The latter is in exact resonance with the uppermost state of an extraction cascade consisting itself of a series of quantum wells. These wells have thicknesses that result in a series of quantized states being separated by roughly one LO-phonon energy. The arrangement of the stages, each of which designed to detect at a different wavelength, was chosen in such a way as to guarantee a flow of electrons from higher lying toward lower lying ground states: the stage with the highest transition energy was grown first (just on top of the bottom contact layer), while the one with the lowest transition energy sat just underneath the top contact layer. The 26 stages have been arbitrarily divided into six groups containing three/five/five/five/five/three stages. Within each group, essentially the same extraction region was used, while the main well thickness was slightly varied. A typical layer sequence of each group is shown in Table I. Fabrication relied on chemical wet etching of square-shaped mesas down to the bottom contact layer using aged etch ($HBr:H_2O_2:H_2O/10:4:1$) and subsequent top and bottom contact metallization (Ti/Ge/Au/Ag/Au, 1.5/12/27/50/250 nm). After a contact anneal at 370 °C for 60 s, a 45° wedge was polished and the sample was mounted on a copper heatsink. The sizes of the square mesas were 100, 200, and 300 μm. These structures were then wire bonded to larger contact pads in order to facilitate handling of the finished devices.

Optical and electrical characterization was performed in a liquid He-flow cryostat equipped with ZnSe windows. A series of *I-V* curves as a function of temperature is presented in Fig. 1. The resistance at around 0 V bias decreases by nearly six orders of magnitude from 3.1×10^8 Ω at 10 K to 833 Ω at 300 K. An Arrhenius plot of the device resistance as a function of inverse temperature revealed an activation energy of 207 meV. Amounting to about 80% of the expected highest optical transition energy (269 meV) minus the

TABLE I. Thicknesses of six typical stages of the QCD in angstroms. Bold numbers stand for InAlAs barriers, and roman numbers stand for InGaAs wells. Underlining mean doping density according to the following list in 10^{17} cm^{-3}: A (4.0), B (3.6), C (3.3), D (3.0), E (2.7), and F (2.5).

A (269 meV): <u>51</u>/**75** // 12.5/**65** // 14.5/**64** // 17/**79** // 20/**77** // 24/**75** // 29/**71** // 35/**68**

B (250 meV): <u>56</u>/**65** // 15.3/**48** // 17.5/**59** // 21/**57** // 25/**65** // 30/**61** // 36/**78**

C (228 meV): <u>61.5</u>/**62** // 18/**48** // 21/**57** // 25/**65** // 30/**61** // 36/**78**

D (209 meV): <u>67</u>/**60** // 20.7/**47** // 24/**55** // 29/**51** // 34/**48** // 42/**55**

E (188 meV): <u>74</u>/**60** // 24.1/**47** // 28/**55** // 33/**51** // 39/**48** // 47/**55**

F (168 meV): <u>81.5</u>/**60** // 27.8/**47** // 34/**55** // 42/**51** // 55/**48**

a)Electronic mail: daniel.hofstetter@unine.ch.
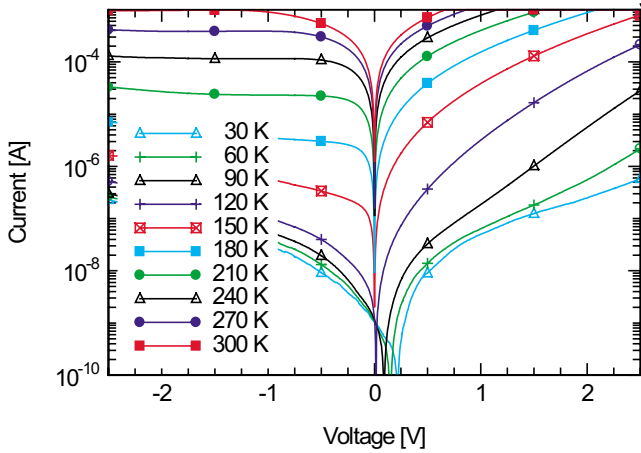b)Present address: National Institute of Standards and Technology, Boulder, CO.

FIG. 1. (Color online) *I-V* curves as a function of temperature measured between 30 and 300 K in steps of 30 K for a 200×200 μm^2 device. All data were obtained under dark conditions.

FIG. 3. (Color online) (a) Absorbance spectra as a function of photon energy at temperatures of 10, 100, 200, and 300 K. (b) Photovoltage spectra as a function of photon energy for temperatures of 10, 100, 200, and 300 K.

Fermi energy of the doping (10 meV), this activation energy shows a too small value, similar to the ones of earlier QCDs. Similarly as mentioned in Ref. 7, its size is determined by a current leakage path, which makes use of an extractor state lying 207 meV above the ground state and having a sufficiently good overlap with the ground states of the neighboring active region periods.

Figure 2 shows spectral responsivity under polarized excitation as a function of photon energy for different temperatures ranging from 10 up to 325 K. Especially at low temperatures, a dip is visible at roughly 1800 cm^{-1}. If we compare the measured responsivity curves with a simulated one, then we can clearly see that this reponsivity gap at around 1850 cm^{-1} was expected from design already. At this photon energy, a smoother overlap between absorption curves of adjacent active region stages could have been achieved by adding one or two supplemental stages. At 10 K, the responsivity peaks at 13 mA/W and 1950 cm^{-1} (E =242 meV). The full width at half maximum at this low temperature is 420 cm^{-1} (ΔE=52 meV, and $\Delta E/E$=21.5%). The surprisingly high responsivity value (2.5 times higher
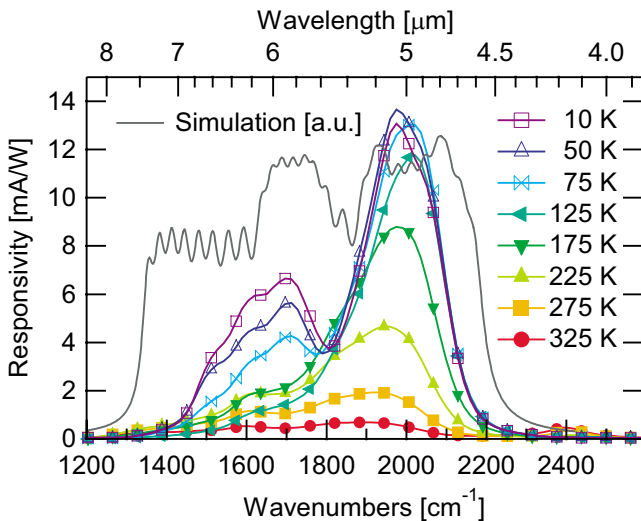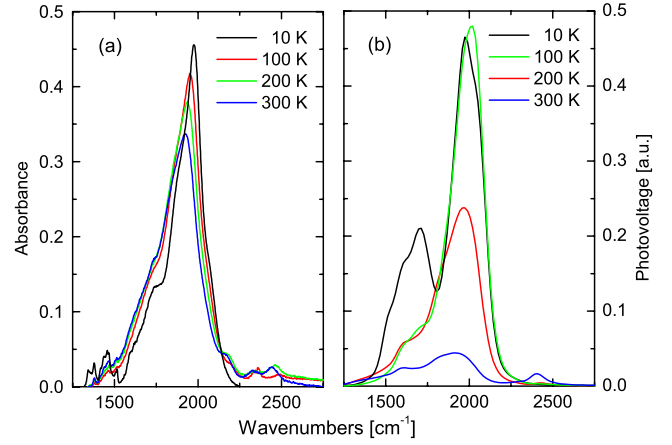

FIG. 2. (Color online) Spectral responsivity as a function of photon energy for different temperatures ranging from 10 up to 325 K compared to a simulated absorption shape assuming equal efficiency and a Lorentzian lineshape with a relative width of 5% for each stage.

than predicted by the simple formula outlined in Ref. 4) can be understood if one considers that within a certain wavelength range, not all periods respond equally to the incoming radiation. Obviously, the signal size increases if, for instance, only 7 instead of 26 periods contribute to the signal. The characterization using a single-mode QC laser showed clearly that such a mode of functioning is indeed possible: all "unused" periods simply act as resistors. When approching room temperature, we still observe a responsivity of 1.25 mA/W peaking at 1920 cm^{-1} (E=238 meV), with a full width at half maximum of 525 cm^{-1} (ΔE=65 meV, and $\Delta E/E$=27.3%). At 300 K, the dip at 1800 cm^{-1} disappears almost completely. If we take—somewhat arbitrarily—the 10% response values at 300 K, then we obtain a wavelength coverage ranging from 4.7 to 7.4 μm. In order to get a valid estimate of the detector performance, we also measured its absorption spectrum at different temperatures using a multi-pass zigzag waveguide configuration. In Fig. 3(a), we present the results of this experiment along with the photovoltages [Fig. 3(b)] measured at 10, 100, 200, and 300 K. At temperatures above 200 K, an additional small photovoltage peak at 2400 cm^{-1} shows up. The activation energy of this feature as extracted from an Arrhenius plot is 74 meV. Together with a Fermi energy of the Si doping of 8 meV, we conclude that the ground state for this transition must lie 82 meV higher than the ground state containing the dopant. Band structure calculations show that for the stages detecting between 6.5 and 7.2 μm, the ground state of the third thinnest extractor well is indeed 82 meV above the ground state of the stage's main well. In addition, the first excited state of the aforementioned extractor well lies 300 meV (2400 cm^{-1}) above its ground state and is in close resonance with the second excited state of the main well. The feature at 2400 cm^{-1} can thus be explained by pure band structure effects. As an interesting observation and despite a nearly constant sheet carrier density through all stages, there is a pronounced decrease in both the absorption and the photovoltage signal at smaller photon energy. Most likely, a smaller resistance of stages detecting at small photon energy, as already observed in spectrally narrow QCDs, is partly responsible for this effect.

From the maximum absorbance (45%) in a 15 double-pass absorption sample, we estimate an absorption of nearly 3% per double pass. Based on a computation using Fermi's
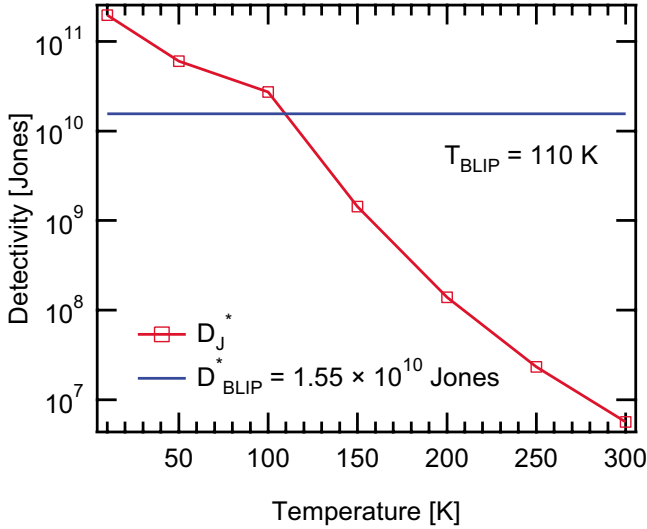
FIG. 4. (Color online) Detectivity as a function of temperature along with a calculated value of the background limited detectivity.

FIG. 5. (Color online) Transmission of a sapphire wafer measured with broadband QCD at 300 K (solid line with symbols, right y-axis, top x-axis). Detector response to illumination with a 5.18 μm quantum cascade laser (solid lines, 10, 100, 200, and 300 K, left y-axis bottom x-axis).

golden rule and the nominal doping levels, we expected only about 1% absorption per double pass. However, linewidth broadening on the order of $\Delta \nu / \nu = 5\%$ has resulted in a considerable overlap between the absorption curves of the single stages and led to this enlarged overall absorption.

From the series of I-V curves shown in Fig. 1, we extracted Johnson noise limited detectivity values, as presented in Fig. 4. They range from 2.0×10^{11} Jones at 10 K to 5.6 $\times 10^6$ Jones at room temperature. The background limited detectivity of this device, D^*_{BLIP}, was determined indirectly under the assumption of a hemispherical field of view and by taking into account the measured responsivity spectra. This theoretical detectivity value is not influenced by the fact that at a certain wavelength not all active region periods contribute to the total signal. D^*_{BLIP} is reached at a temperature $T_{BLIP} = 110$ K and amounts to 1.55×10^{10} Jones. In Fig. 5, we finally present two measurements, which prove that such a device can work well although transport through the structure would in theory be problematic due to the lack of the necessary 26 different incident photon energies. In the first experiment, the transmission of a sapphire window was determined, while in the second, the detector response under illumination with a single-mode continuous wave quantum cascade laser emitting at 5.18 μm was measured. In the absorption experiment, we compared the detector response with and without a sapphire window and saw a sharp drop in the responsivity at 1500 cm^{-1}. When dividing the two curves, we obtained a typical transmission curve for sapphire with an absorption edge at roughly 1600 cm^{-1}. As shown in Fig. 5, this transmission actually drops from near 80% down to below 10% (line with symbols). In the other experiment, a quantum cascade laser was aligned to the Fourier spectrometer and focused onto the detector. A response with a high signal-to-noise ratio could be obtained for all detector tem-
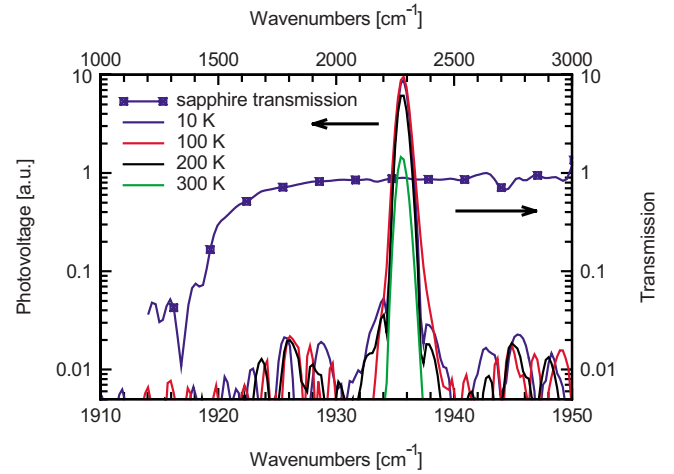
peratures between 10 and 300 K, thus proving the concept of the broadband QCD. This is true even for low temperatures where the large QCD resistance leads to a much poorer conductivity of the entire device.

In conclusion, we have presented a midinfrared QCD with a spectrally broad responsivity between 7.4 and 4.7 μm. A relative linewidth (full width at half maximum) of 27.3% was seen at room temperature. A background limited operating temperature of 110 K with a detectivity of 1.55×10^{10} Jones and maximum responsivities of 13 mA/W at 10 K and 1.25 mA/W at 300 K have been demonstrated. This device is an important step toward semiconductor based intersubband detectors for spectrally broad applications such as spectroscopy.

[1] L. Gendron, M. Carras, A. Huynh, V. Ortiz, C. Koeniguer, and V. Berger, Appl. Phys. Lett. **85**, 2824 (2004).

[2] L. Gendron, C. Koeniguer, V. Berger, and X. Marcadet, Appl. Phys. Lett. **86**, 121116 (2005).

[3] D. Hofstetter, M. Graf, T. Aellen, J. Faist, L. Hvozdara, and S. Blaser, Appl. Phys. Lett. **89**, 061119 (2006).

[4] M. Graf, N. Hoyler, M. Giovannini, J. Faist, and D. Hofstetter, Appl. Phys. Lett. **88**, 241118 (2006).

[5] F. R. Giorgetta, E. Baumann, D. Hofstetter, C. Manz, Q. Yang, K. Köhler, and M. Graf, Appl. Phys. Lett. **91**, 111115 (2007).

[6] M. Graf, G. Scalari, D. Hofstetter, J. Faist, H. Beere, E. Linfield, D. Ritchie, and G. Davies, Appl. Phys. Lett. **84**, 475 (2005).

[7] F. R. Giorgetta, E. Baumann, R. Théron, M. L. Pellaton, D. Hofstetter, M. Fischer, and J. Faist, Appl. Phys. Lett. **92**, 121101 (2008).

[8] See, for instance. http://www.judsontechnologies.com/mercadm.htm.